

We are IntechOpen, the world's leading publisher of Open Access books Built by scientists, for scientists

6,900

Open access books available

186,000

International authors and editors

200M

Downloads

Our authors are among the

154

Countries delivered to

TOP 1%

most cited scientists

12.2%

Contributors from top 500 universities



WEB OF SCIENCE™

Selection of our books indexed in the Book Citation Index
in Web of Science™ Core Collection (BKCI)

Interested in publishing with us?
Contact book.department@intechopen.com

Numbers displayed above are based on latest data collected.
For more information visit www.intechopen.com



Biocompatibility and Antimicrobial Activity of Some Quaternized Polysulfones

Silvia Ioan and Anca Filimon

*"Petru Poni" Institute of Macromolecular Chemistry Iasi
Romania*

1. Introduction

In recent decades, considerable attention has been devoted to the investigation of new applications of polysulfones, which are mainly because of their specific properties. The literature shows that polysulfones and their derivatives are widely used as new functional materials in biochemical, industrial, and medical fields because of their structure and physical properties, such as their good optical properties, high thermal and chemical stability, mechanical strength, resistance to extreme pH values, and low creep (Barikani & Mehdipour-Ataei, 2000; Higuchi et al., 1988; Johnson, 1969; Mann & West, 2001). The chain rigidity is derived from the relatively inflexible and immobile phenyl and SO₂ groups, whereas their toughness is derived from the connecting ether oxygen. Although these materials have excellent overall properties, their intrinsic hydrophobic nature precludes their use in membrane applications, which require a hydrophilic character. Therefore, such polymers should be modified to improve their performance for specific applications (Johnson, 1969; Khang et al., 1995). The chemical modification of polysulfones, especially the chloromethylation reaction, is a subject of considerable interest from both theoretical and practical points of view; there is interest in obtaining the precursors for functional membranes, coatings, ion exchange resins, ion exchange fibers, and selectively permeable membranes (Higuchi et al., 2002; Tomaszewska et al., 2002). Functionalized polymers, chloromethylated and quaternized polysulfones, have evidenced several interesting properties, which recommend them for a wide range of industrial and environmental applications. Quaternization with ammonium groups is an efficient method for increasing their hydrophilicity. Accordingly, these polymers can be used for multiple applications, e.g. as biomaterials and semipermeable membranes. Also, the different components of a block or graft copolymer may segregate in bulk to yield nanometer-sized patterns or mesophasic structures. Numerous applications involve nanodomained solids. By matching the periodicity of the patterns with the wavelength of visible light, literature studies have demonstrated that block copolymers, including polysulfones, act as photonic crystals. Segregated block copolymers, polysulfones included, have been also used as precursors for the preparation of various nanostructures, including nanospheres, nanofibers, nanotubes, and thin membranes-containing nanochannels. Thin membranes containing nanochannels have been used as membranes, pH sensors, or templates for the preparation of metallic nanorods. Furthermore, in the last decades, blends of polysulfone or modified polysulfones

and other synthetic polymers have continued to be a subject of intense both academic and industrial investigation, because of their simplicity and effectiveness in the mixture of two different polymers for producing new materials.

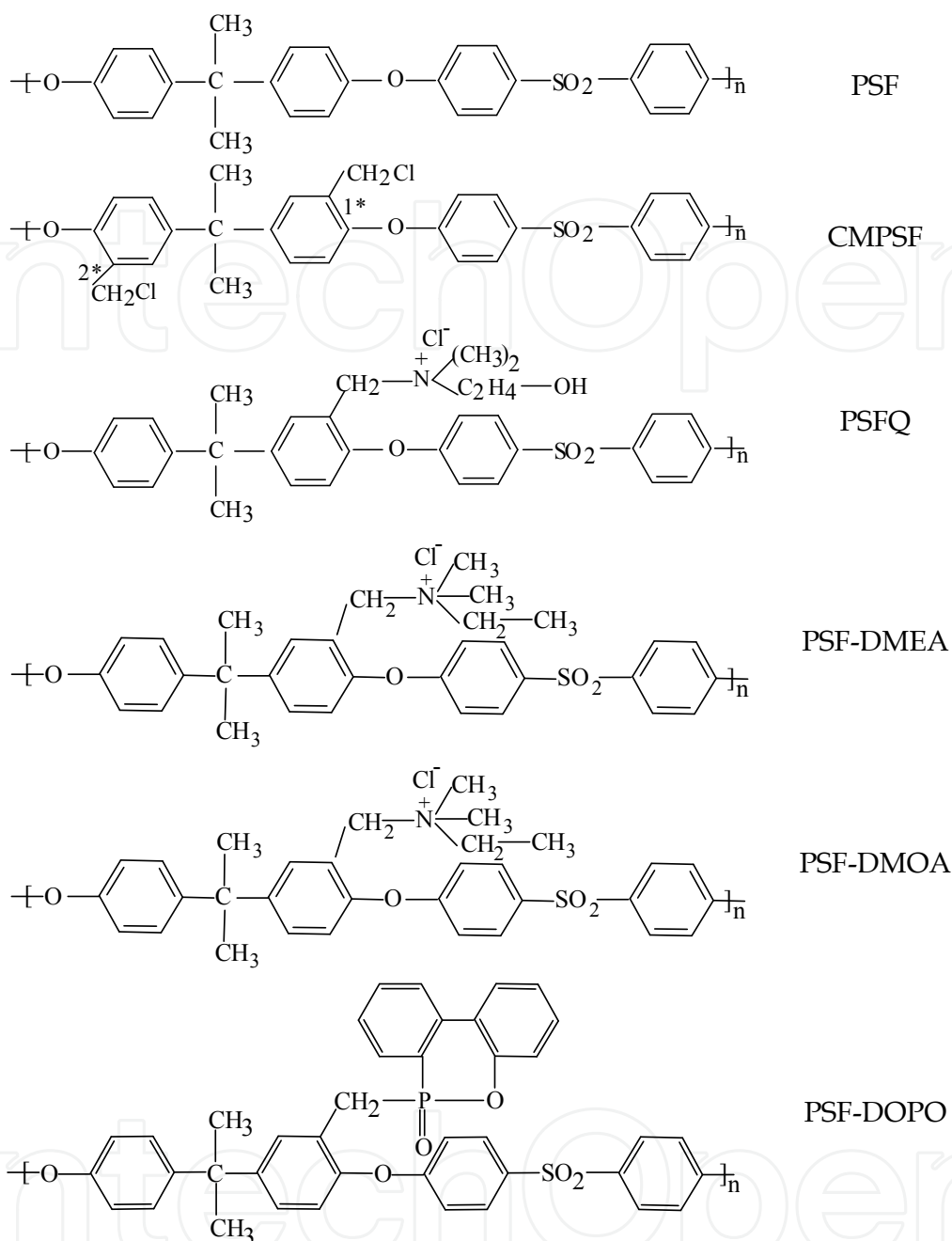
In such applications, the addition of functional groups to the polysulfone enhance some properties of the material, such as hydrophilicity (which is of special interest for biomedical applications) (Guan et al., 2005), antimicrobial action (Filimon et al., 2009; Yu et al., 2007), and solubility characteristics (Filimon et al., 2007; Ioan et al., 2006), to allow higher water permeability and better separation (Idris et al., 2007; Kochkodan et al., 2008). In addition, functional groups are an intrinsic requirement for affinity, ion exchange, and other specialty membranes (Guiver et al., 1993).

In this context, the paper presents the synthesis and some properties of new polysulfones for biomedical applications. Studies are carried out on the quaternization reaction of chloromethylated polysulfones with N,N-dimethylethanolamine (Filimon et al., 2010; Ioan et al., 2006a, 2006b, 2007), N,N-dimethylethylamine and N,N-dimethyloctylamine (Ioan et al., 2011a), for obtaining water soluble polymers with various amounts of ionic chlorine, or on the new polysulfones with bulky phosphorus pendant groups, obtained by chemical modification of the chloromethylated polysulfones by reacting the chloromethyl group with the P-H bond of 9,10-dihydro-oxa-10-phosphophenanthrene-10-oxide (Ioan et al., 2011b).

The different properties, such as morphological aspect (by atomic force microscopy), where the type of nonsolvents in casting solutions of polymer (identified by viscometry and rheology investigations (Ioan et al., 2006b; Filimon et al., 2010)) significantly influenced membrane morphology and where ordered domains depend on the charge density of polyelectrolytes, the hydrophilic/hydrophobic characteristics (by contact angle method), as well as the history of the formed films, correlated with a good adhesion of the red blood cells and with a good cohesions of the platelets on the surface of the quaternized polysulfone films (determined from surface properties), are investigate for specific biomedical applications. Furthermore, bacterial adhesions to the surfaces (by analyzing the inhibition zones) are studied for applications of modified polysulfones as semipermeable membranes. Thus, the analysis of antibacterial activity, using *Escherichia coli* ATCC 10536 and *Staphylococcus aureus* ATCCC 6538 microorganisms, contribute to extending the possible applications of quaternized polysulfones membranes in biomedical domains.

2. Synthesis of some new functionalized polysulfones

The quaternized polysulfones tested for biomedical applications, such as PSFQ, PSF-DMEA and PSF-DMOA, are obtained by quaternized reaction (Luca et al., 1988) of chloromethylated polysulfones (CMPSF) with N,N-dimethylethanolamine (Filimon et al., 2010; Ioan et al., 2006a, 2006b, 2007;), N,N-dimethylethylamine, and N,N-dimethyloctylamine (Ioan et al., 2011a), respectively. Also, polysulfones with bulky phosphorus pendant groups (PSF-DOPO) are obtained by chemical modification of the chloromethylated polysulfone, performed by reacting the chloromethyl group with the P-H bond of 9,10-dihydro-oxa-10-phosphophenanthrene-10-oxide (DOPO) (Petreus et al., 2010). The general chemical structures of the studied polysulfones, PSF, CMPSF and quaternized polysulfones PSFQ, PSF-DMEA, PSF-DMOA and PSF-DOPO are presented in Scheme 1.



Scheme 1. Chemical structures of polysulfone (PSF), chloromethylated polysulfone (CMPSF), quaternized polysulfones (PSFQ, PSF-DMEA, PSF-DMOA) and polysulfone with bulky phosphorus pendant groups (PSF-DOPO)

Table 1 lists the chlorine content, substitution degree, molecular weights of the structural units, m_0 , number-average molecular weights, M_n , and intrinsic viscosities determined in *N,N*-dimethylformamide (DMF) at 25°C of polysulfone and chloromethylated polysulfones (Ioan et al., 2006a). The characteristics of quaternized polysulfones PSFQ1 and PSFQ2 (Ioan et al., 2006b), and also PSF-DMEA and PSF-DMOA (Filimon et al., 2010) are presented in Table 2.

Samples	Cl, %	DS	m_0	M_n	$[\eta]$, dL/g
PSF	0	0	442.51	39000	0.3627
CMPSF1	3.34	0.437	463.68	41000	0.3929
CMPSF2	10.53	1.541	517.17	46000	0.4703
CMPSF3	12.13	1.828	530.83	47000	0.6970

Table 1. Chlorine content, substitution degree, DS, molecular weights of the structural units, m_0 , number-average molecular weights, M_n , and intrinsic viscosities in DMF at 25°C, $[\eta]$, of polysulfone and chloromethylated polysulfones

Samples	Obtained from:	Cl _i , %	m_0	M_n
PSFQ1	CMPSF1	2.15	479.47	42000
PSFQ2	CMPSF2	5.71	647.31	57000
PSFQ3	CMPSF3	6.21	691.29	61000
PSF-DMEA	CMPSF2	2.89	551.70	49000
PSF-DMOA	CMPSF2	3.23	627.30	56000

Table 2. Ionic chlorine content, Cl_i, molecular weights of the structural units, m_0 , and number-average molecular weights, M_n , of quaternized polysulfones

On the other hand, the substitution of chlorine with the bulky cyclic phosphorus compound is carried out at elevated temperature, using a large excess of phosphorus reactant. The reactive P-H group interacts with CH₂Cl group of chloromethylated polysulfone. The occurrence of HCl evolved from the reaction proved the substitution.

Samples	Elemental composition, %					DS	m_0^*	M_n
	C	H	S	O	Cl			
PSF	73.07	5.12	7.47	14.16	0.18	-	443	39000
CMPSF1	68.81	4.81	6.96	15.22	4.20	0.56	470	41000
CMPSF2	66.58	4.68	6.72	15.44	6.58	0.90	486	43000
CMPSF3	61.27	4.25	6.12	17.86	10.50	1.53	528	47000

Table 3. Carbon, hydrogen, sulfur, oxygen and chlorine content, substitution degree, DS, molecular weight of the structural units, m_0 , and number-average molecular weights, M_n , of polysulfone and chloromethylated polysulfone

Also, the chloromethylation reaction of polysulfone may occur in position 1* for CMPSF1 and CMPSF2, when DS < 1. Thus, according to Table 1, the difference between these two samples lies in the different values of the chlorine content. For sample CMPSF3 with DS > 1, the chloromethylation reaction occurs in positions 1* and 2*. Table 3 lists the carbon, hydrogen, sulfur, oxygen and chlorine content, degree of substitution, molecular weights of the structural units, m_0 , and number-average molecular weight, M_n , of the chloromethylated polysulfones, determined from the polymerization degree of the polysulfone (DP \cong 88) and molecular weights of the structural units of chloromethylated polysulfones (Petreus et al. 2010).

The characteristics of phosphorus-modified polysulfones are presented in Table 4 (Ioan *et al.*, 2011b).

Samples	Obtained from:	Elemental composition, %						DS	m_0	M_n
		C	H	S	O	Cl	P			
PS-DOPO-1	CMPSF1 (4.2 Cl %)	72.5	4.9	5.7	13.6	0.4	2.9	0.59	491.5	43000
PS-DOPO-2	CMPSF2 (6.6 Cl %)	71.3	4.7	5.2	14.4	0.4 ₅	3.4	0.72	569.4	50000
PS-DOPO-3	CMPSF3 (10.5 Cl %)	71.1	4.3	4.5	13.7	0.3 ₅	6.0	1.85	975.0	90000

Table 4. Elemental composition, substitution degree, DS, molecular weight of the structural units, m_0 , and number-average molecular weights, M_n , of phosphorus modified polysulfones

3. Role of casting solutions on the functionalized polysulfones surface morphology

Some studies have reported that the chain shape of a polymer in solution could affect the morphology of the polymer in bulk (Hopkins *et al.*, 2006; Huang *et al.*, 2000; Qian *et al.*, 2005). The PSFQ membranes used in atomic force microscopy (AFM) are prepared with different solvent mixtures, including DMF/MeOH, DMF/water, MeOH/DMF and MeOH/water. The solvent systems are selected as a function of the ionic chlorine content of PSFQ. Thus, DMF solvates PSFQ1 with an ionic chlorine content of 2.15% more intensely than the mixed DMF/MeOH and DMF/water solvents with high contents of MeOH and water, respectively. On the other hand, MeOH solvates PSFQ2 with an ionic chlorine content of 5.71%, more strongly than the mixed MeOH/DMF and MeOH/water solvents with high contents of DMF and water, respectively (Filimon *et al.*, 2007); Ioan *et al.*, 2006b). AFM is used to examine film surface and to measure their surface topography. All of the images presented in Figures 1-3 are recorded under ambient conditions, at different size scales to provide morphological details. Each micrograph shows that the membrane surface is not smooth, existing in ordered domains, in which are distributed pores and nodules of different size and intensities. Increasing the nonsolvent content in the casting solutions favors modification of the ordered domains, more visibly in images with a 500 nm x 500 nm or 3 μ m x 3 μ m scanning area. Thus, the average surface roughness in the 3 μ m x 3 μ m scanning area decreases from 0.354 nm for the PSFQ1 membranes obtained in 60 DMF/40 MeOH (Figure 1 (1b, b'), in two-dimensional (2D) and three-dimensional (3D) AFM images, respectively), to 0.193 nm for the PSFQ1 membranes realized in 20 DMF/80 MeOH (Figure 1 (2b, b'), in 2D and 3D AFM images, respectively). Also, the AFM images from Figure 1, for a more extended scanning area, show that increasing the nonsolvent content favors the increase of the pores number and of their characteristics, such as area, volume, diameter, and also root-mean-square roughness of the surface (rms),

whereas their depth decreases. This changing trend in morphology is probably due to the modification of the chain conformation of quaternized polysulfones, which is influenced by the quality of the mixed solvents (Qian et al., 2005; Kesting, 1990).

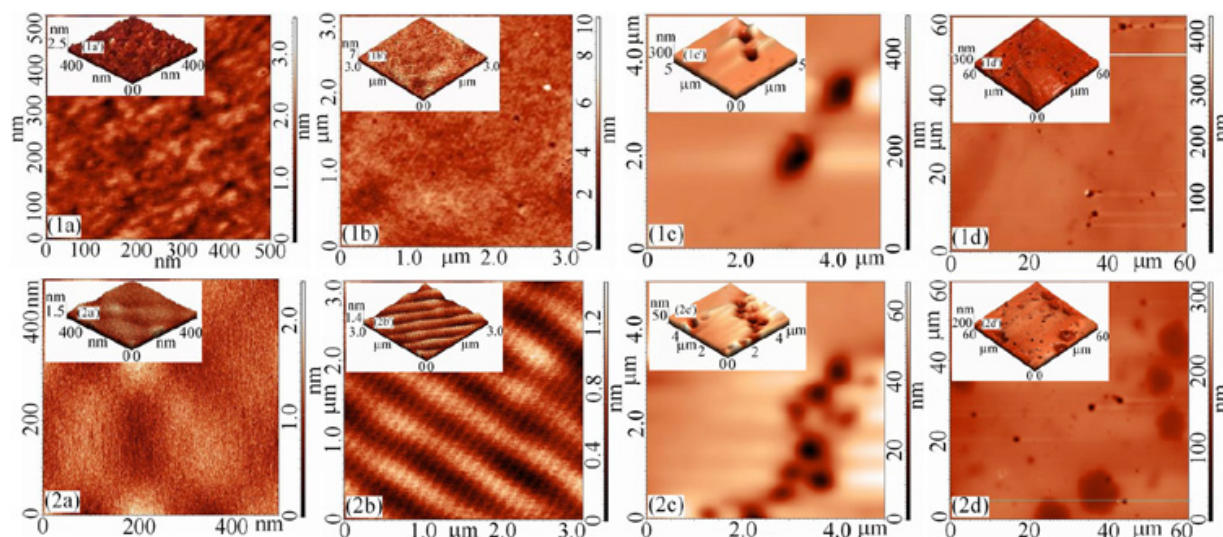


Fig. 1. AFM images of PSFQ1 membranes obtained from different DMF/MeOH solvent mixtures. (1) 60/40 DMF/MeOH: (a, a') 2D and 3D images - scanned area 500 nm x 500 nm , (b, b') 2D and 3D images - scanned area 3 μm x 3 μm , (c, c') 2D and 3D images - scanned area 5 μm x 5 μm , (d, d') 2D and 3D images - scanned area 60 μm x 60 μm ; (2) 20/80 DMF/MeOH: (a, a') 2D and 3D images - scanned area 500 nm x 500 nm , (b, b') 2D and 3D images - scanned area 3 μm x 3 μm , (c, c') 2D and 3D images - scanned area 5 μm x 5 μm , (d, d') 2D and 3D images - scanned area 60 μm x 60 μm

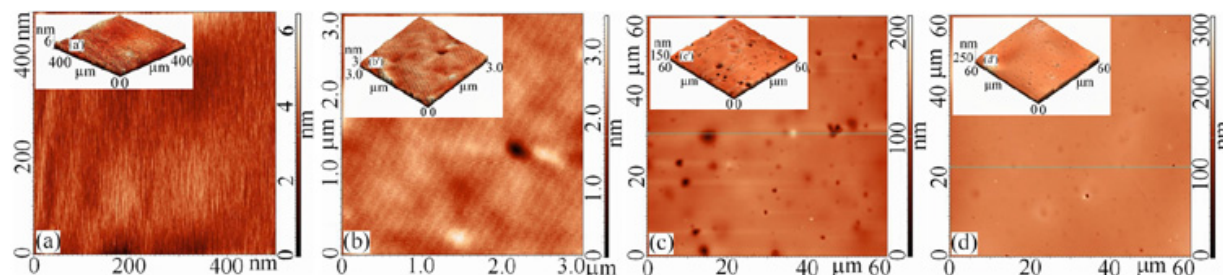


Fig. 2. AFM images of PSFQ1 membranes obtained from: (a, a') 60/40 DMF/water, 2D and 3D images - scanned area 500 nm x 500 nm ; (b, b') 60/40 DMF/water, 2D and 3D images - scanned area 3 μm x 3 μm ; (c, c') 60/40 DMF/water, 2D and 3D images - scanned area 60 μm x 60 μm ; (d, d') 40/60 DMF/water, 2D and 3D images - scanned area 60 μm x 60 μm

A higher charge density in PSFQ2 determines the appearance of nodules, as illustrated in Figure 3 (a, a' and b, b') . The presence of water as a nonsolvent in solutions used for casting membranes influences the AFM images; increasing the water content leads to lower area pores for both polymer membranes under study (Figure 2 (c, c' and d, d') for PSFQ1 membranes, and Figure 3 (c, c' and d, d') for PSFQ2 membranes) and to a lower number of nodules in the PSFQ2 membranes (Figure 3 (c, c' and d, d')). In addition, it may be assumed

that the association phenomena of MeOH and water over different composition domains of their mixtures might be one of the factors affecting the morphology of the PSFQ2 membrane surface. Thus, mixed solvents are formed from water and MeOH associated with water, at high water contents; in contrast, at high MeOH compositions, the mixtures consist largely of MeOH and water associate with MeOH. These phenomena change the PSFQ2 solubility, and determine the modification of the solution properties (Filimon et al., 2007), as well as morphology - Figure 3 (c, c' and d, d').

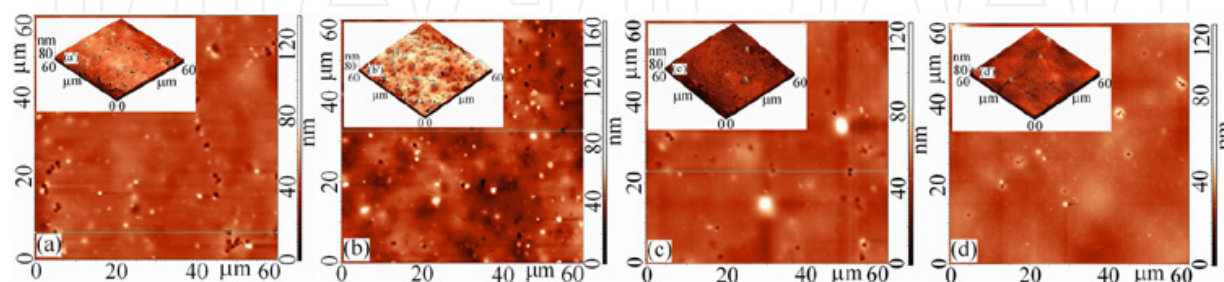


Fig. 3. AFM images of PSFQ2 membranes at scanned area $60 \mu\text{m} \times 60 \mu\text{m}$, obtained from: (a, a') 2D and 3D images, 60/40 MeOH/DMF; (b, b') 2D and 3D images, 20/80 MeOH/DMF; (c, c') 2D and 3D images, 60/40 MeOH/water; (d, d') 2D and 3D images, 20/80 MeOH/water

Table 5 gives the average values of the pore characteristics and surface roughness parameters of membranes prepared from different solvent/nonsolvent mixtures. On the other hand, obviously, the number of nodules from the AFM images of the PSFQ2 membranes increases as the nonsolvent content increases.

Samples	Cast solvents	Pore characteristics				Surface roughness		
		Area	Vol.	Depth	Diameter	rms	nhp	nhh
PSFQ1	60/40 DMF/MeOH	0.499	74.72	237.62	0.793	12.36	279	253
	20/80 DMF/MeOH	1.441	83.47	88.54	1.350	18.36	205	180
	60/40 DMF/water	0.342	8.85	46.21	0.665	8.83	170	135
	40/60 DMF/water	0.165	4.60	45.74	0.460	6.53	200	190
PSFQ2	60/40 MeOH/DMF	0.186	1.00	6.82	0.489	5.45	66	50
	20/80 MeOH/DMF	0.216	0.88	6.99	0.528	5.62	64	42
	60/40 MeOH/water	0.485	5.84	20.07	0.783	9.72	104	50
	20/80 MeOH/water	0.145	0.25	3.01	0.431	2.72	45	30

Table 5. Pore characteristics including the area ($\mu\text{m} \times \mu\text{m}$), volume ($\mu\text{m} \times \mu\text{m} \times \text{nm}$), depth (nm), and diameter (μm), and surface roughness parameters including the root-mean-square roughness (rms, nm), nodule height from the height profile (nhp, nm), and nodule average height from the histogram (nhh, nm) of membranes prepared from the PSFQs with different solvent mixtures

On the other hand, Figures 4 and 5 exemplify the bi- and three-dimensional structures evidence by AFM investigations of PSF-DMEA films prepared with 100/0, 75/25, 50/50 and 25/75, and also with 75/25, 50/50 and 40/60 of DMF/MeOH and DMF/water compositions

solvent mixtures, respectively. According to the AFM images, increasing the nonsolvent content in the casting solutions favors modification of surface morphology.

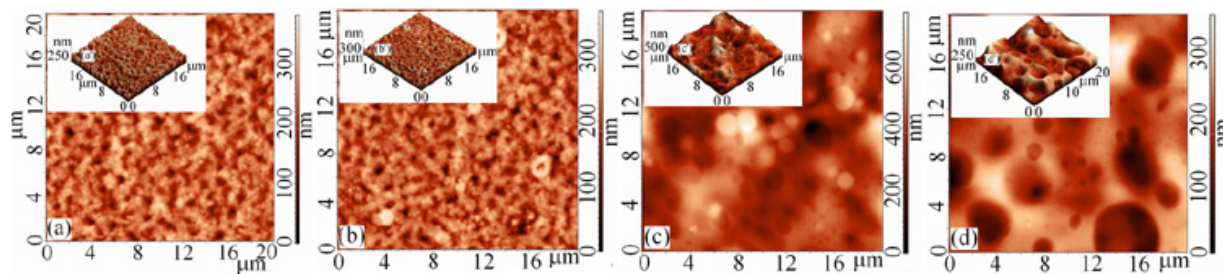


Fig. 4. 2D and 3D AFM images with $20 \times 20 \mu\text{m}^2$ scanned areas of the PSF-DMEA films obtained from DMF/MeOH solutions: (a, a') - 100/0; (b, b') - 75/25; (c, c') - 50/50; (d, d') - 25/75

Thus, Figure 4 and Table 6 show that average surface roughness attains a maximum value at 50/50 DMF/MeOH, and favors the appearance of the smallest number of pores with highest depth values. Also, the area, diameter, length and mean width increase with increasing the nonsolvent content. It should be noted that the thermodynamic quality of the solvent mixtures over the studied domain increases with the addition of nonsolvent, at approximately 50/50 DMF/MeOH becoming constant, while the preferential adsorption of nonsolvent takes a maximum value, according to literature data (Filimon et al., 2010). In addition, the presence of water as a nonsolvent in the solutions used for casting films influenced the AFM images presented in Figure 5; a higher water content decreases the thermodynamic quality of the DMF/water solvent mixtures so that, at 50/50 DMF/water, a minimum value of surface roughness and a maximum number of pores with minimum values of area, depth, diameter, length and mean width, are observed.

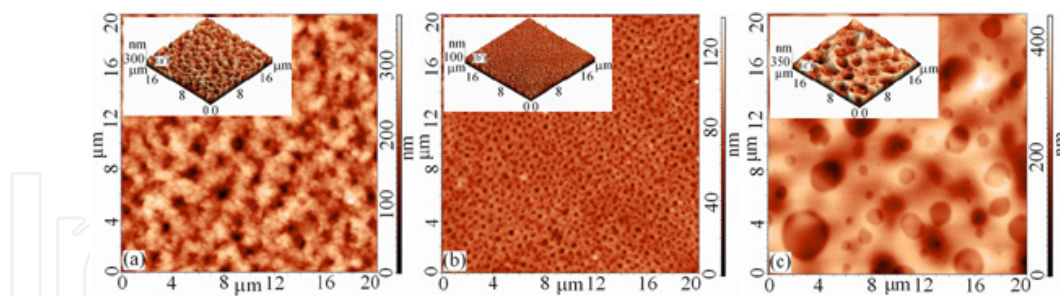


Fig. 5. 2D and 3D AFM images with $20 \times 20 \mu\text{m}^2$ scanned areas of the PSF-DMEA films obtained from DMF/water solutions: (a, a') - 75/25; (b, b') - 50/50; (c, c') - 40/60

Figure 6 plot also two- and three-dimensional structures of PSF-DMOA films prepared with DMF/MeOH solvent mixtures of various compositions (100/0, 75/25, 50/50, and 45/55). According to these images, increasing the nonsolvent content in the casting solutions favors modification of the surface morphology. Thus, the average surface roughness decreased with increasing MeOH content and favors increases in the pore number and pore characteristics (area, depth, diameter, and mean width) according to Table 6. The thermodynamic quality of solvent mixtures over the studied domain increases with the addition of the nonsolvent (Filimon et al. 2010; Ioan et al., 2011a).

Solvent mixtures	Pore characteristics						Surface roughness		
	Number of pores	Area	Depth	Diameter	Length	Mean width	Sa	rms	nhh
PSF-DMEA, DMF/MeOH									
100/0	234	0.24	272.78	0.57	0.86	0.31	33.97	42.87	231.14
75/25	268	0.27	259.59	0.62	0.94	0.32	31.89	41.47	217.26
50/50	52	0.47	348.25	0.78	1.09	0.47	74.09	95.12	402.61
25/75	37	1.10	242.07	1.18	1.73	0.62	48.36	59.80	193.33
PSF-DMEA, DMF/water									
75/25	147	0.51	245.19	0.86	1.25	0.48	37.41	47.76	227.79
50/50	1080	0.06	89.57	0.23	0.47	0.15	6.87	9.27	77.43
40/60	42	2.19	230.10	1.64	2.43	0.86	44.98	57.61	281.80
PSF-DMOA, DMF/MeOH									
100/0	9	10.43	25.64	3.33	6.24	1.45	14.11	16.82	58
75/25	-	-	-	-	-	-	14.43	19.90	82
50/50	34	0.70	11.37	0.89	1.56	0.42	3.09	4.41	17
45/55	44	0.80	16.02	0.98	1.53	0.49	2.77	4.24	28
PSF-DMOA, DMF/water									
75/25	5	3.12	13.65	1.97	3.26	0.96	1.59	2.34	15
60/40	27	0.04	19.54	0.22	0.35	0.11	9.19	11.83	70
50/50	18	2.09	5.55	1.46	2.63	0.64	1.52	2.17	8

Table 6. Pore characteristics, including number of pores, area (μm^2), depth (nm), diameter (μm), length (μm), and mean width (μm), and surface roughness parameters, including average roughness (Sa, nm), root mean square roughness (rms, nm), and nodule average height from the histogram (nhh, nm) of PSF-DMEA and PSF-DMOA films prepared from solutions in DMF/MeOH and DMF/water, with $20 \times 20 \mu\text{m}^2$ scanned areas, corresponding to the 2D AFM images (Ioan et al., 2011)

On the other hand, the presence of water as a nonsolvent in the solutions used for casting films influenced the AFM images presented in Figure 7; a higher water content decreased the thermodynamic quality of the DMF/water solvent mixtures.

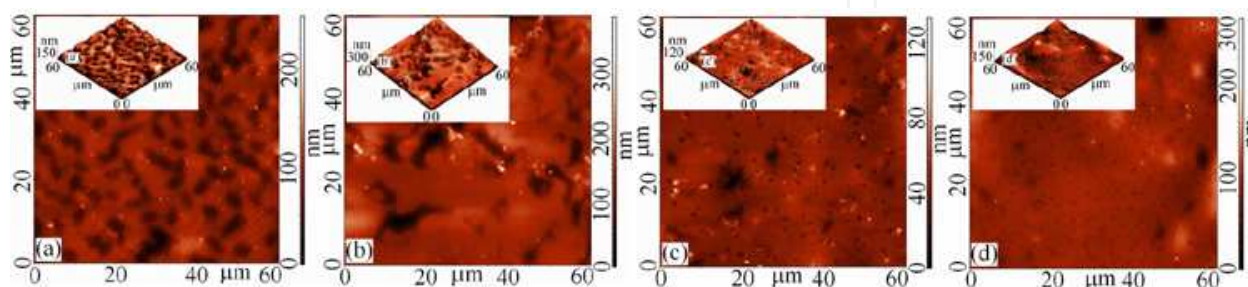


Fig. 6. 2D and 3D AFM images with $60 \times 60 \mu\text{m}^2$ scanned areas of the PSF-DMOA films obtained from DMF/MeOH solution: (a, a') 100/0; (b, b') 75/25; (c, c') 50/50; (d, d') 45/55

Therefore, for a 60/40 DMF/water mixture, the average surface roughness, number of pores, and pore depth are maximum with a minimum area (Table 6). It can be assumed that the specific interactions with the mixed solvents employed in this study modify the PSF-DMOA solubility and determine the modification of the solution properties.

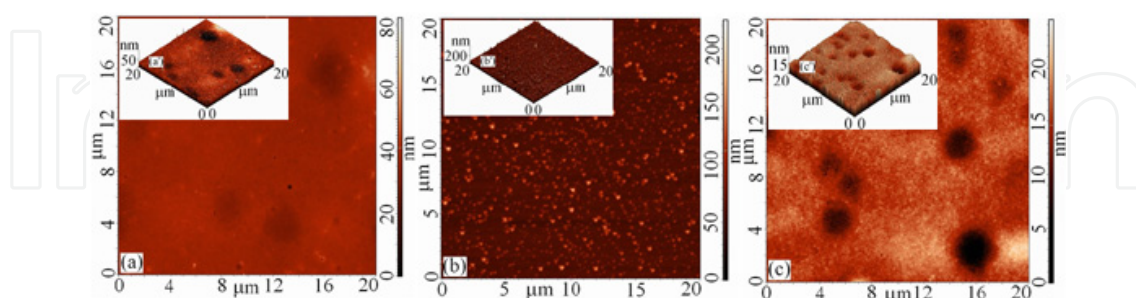


Fig. 7. 2D and 3D AFM images with $20 \times 20 \mu\text{m}^2$ scanned areas of the PSF-DMOA films obtained from DMF/water solution: (a, a') 75/25; (b, b') 60/40; (c, c') 50/50

In the same context, from AFM images (Figure 8) one can see that the bulky phosphorus pendant groups in PSF-DOPO determine the formation of domains with pores in an approximately continuous matrix (Ioan et al., 2011b).

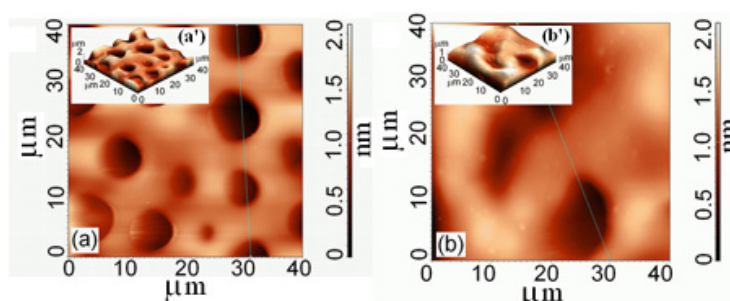


Fig. 8. 2D and 3D-AFM images for PS-DOPO-1 (a, a') and PS-DOPO-2 (b, b')

Samples	Pore characteristics				Surface roughness		
	Area	Volume	Depth	Diameter	rms	nhp	nhh
PS-DOPO-1	23.25	14.39	1.51	5.02	363.16	0.45	1.40
PS-DOPO-2	28.96	15.19	0.95	7.61 6.00*	343.11	0.70	1.30
PS-DOPO-3				25.00*			

* From scanning electron microscopy, according to previous data (Petreus et al., 2010)

Table 7. Pore characteristics including area ($\mu\text{m} \times \mu\text{m}$), volume ($\mu\text{m} \times \mu\text{m} \times \text{nm}$), depth (μm), and diameter (μm), and surface roughness parameters including root-mean-square roughness (rms, nm), and nodules height from the height profile (nhp, μm) and nodules average height from the histogram (nhh, μm) of polysulfone with bulky phosphorus pendant groups membranes obtained from AFM investigations

Pore characteristics (including area, volume, depth, and diameter) and surface roughness parameters (including root-mean-square roughness (rms), and nodules height from the height profile (nhp) from profile analysis, and nodules average height, from the histogram (nhh)), are presented in Table 7. The dimensions of pores increase and their depth decreases with increasing the substitution degrees, so that, for the PS-DOPO-3 sample, the dimensions exceed the limit of the AFM apparatus.

On the other hand, AFM studies support the conclusion that the increasing density of bulky phosphorus pendant groups from the side chain and decreases roughness and, implicitly, confirm poor adhesion of the modified polysulfone films. Also, the bulky phosphorus pendant groups, found in position 1* for samples PS-DOPO-1 and PS-DOPO-2, and in positions 1* and 2* for sample PS-DOPO-3, modify the rigidity and hydrophobicity, and determine different forms of entanglement in polymer solutions, influencing membrane morphology and AFM images.

4. Surface tension parameters

Surface tension parameters of quaternized polysulfones are calculated by the geometric mean method (GM) (equation (1)) (Kälble et al., 1969; Owens et al., 1969) and the acid/base method (LW/AB) (equation (2)) (van Oss et al, 1988a; van Oss et al, 1988b). In this context, the surface tension data of the doubly-distilled water (W), ethylene glycol (EG), glycerol (G) and formamide (FA) used in the calculations of the surface tension parameters of PSFQ are presented in Table 8.

$$\frac{1 + \cos \theta}{2} \cdot \frac{\gamma_{lv}}{\sqrt{\gamma_{lv}^d}} = \sqrt{\gamma_{sv}^p} \cdot \sqrt{\frac{\gamma_{lv}^p}{\gamma_{lv}^d}} + \sqrt{\gamma_{sv}^d}; \gamma_{sv} = \gamma_{sv}^d + \gamma_{sv}^p \quad (1)$$

where θ is the contact angle determined for test liquids, subscripts “lv” and “sv” denote the interfacial tension between liquid-vapor and surface-vapor, respectively, while superscripts “p” and “d” denote the polar and disperse components, respectively, of total surface tension, γ_{sv} .

$$1 + \cos \theta = \frac{2}{\gamma_{lv}} \cdot \left(\sqrt{\gamma_{sv}^{LW} \cdot \gamma_{lv}^{LW}} + \sqrt{\gamma_{sv}^+ \cdot \gamma_{lv}^-} + \sqrt{\gamma_{sv}^- \cdot \gamma_{lv}^+} \right); \gamma_{sv}^{LW/AB} = \gamma_{sv}^{LW} + \gamma_{sv}^{AB} \quad (2)$$

where $\gamma_{sv}^{AB} = 2 \cdot \sqrt{\gamma_{sv}^+ \cdot \gamma_{sv}^-}$, superscript “LW/AB” indicates the total surface tension, and also, superscript “AB” and “LW” represent the polar component obtained from the electron-donor, γ_{sv}^- , and the electron-acceptor, γ_{sv}^+ , interactions, and the disperse component, respectively.

Literature (Della Volpe et al., 2004) shows that an improper utilization of three liquids without dispersive liquids, or with liquids prevalently basic or prevalently acidic, strongly increases the ill-conditioning of the system. In addition, the contact angles should be measured with a liquid whose surface tension is higher than the anticipated solid surface tension (Kwok et al., 2000).

Table 9 shows the contact angle values between water, ethylene glycol, glycerol or formamide and PSF, CMPSF and PSFQ membranes. The surface tension of PSF evidences the lowest hydrophilicity, induced by the aromatic rings connected by one carbon and two methyl groups, oxygen elements, and sulfonic groups, while chloromethylation of PSF with the functional group $-\text{CH}_2\text{Cl}$ increases hydrophilicity (see the values of surface tension for PSF and CMPSF in Table 10). Moreover, the results indicate that the PSFQ membranes are the most hydrophilic ones from the studied samples (lowest water contact angle), due to the N,N-dimethylethanolamine hydrophilic side groups. Hence, it is observed that total surface tension, γ_{sv} or $\gamma_{\text{sv}}^{\text{LW/AB}}$, and the polar component, $\gamma_{\text{sv}}^{\text{p}}$ or $\gamma_{\text{sv}}^{\text{AB}}$, increase with the degree of substitution of CMPSF and with the quaternization degree of the ammonium groups for PSFQ samples.

Test liquids	γ_{lv}	$\gamma_{\text{lv}}^{\text{d}}$	$\gamma_{\text{lv}}^{\text{p}}$	γ_{lv}^-	γ_{lv}^+
Water (W) (Ström et al., 1987; (Rankl et al., 2003))	72.8	21.8	51.0	25.50	25.50
Ethylene glycol (EG) (Yildirim et al., 1997)	48.0	29.0	19.0	47.00	1.92
Glycerol (G) (van Oss et al., 1989)	64.0	34.0	30.0	57.40	3.92
Formamide (FA) (van Oss et al., 1989)	58.0	39.0	19.0	39.60	2.28
Methylene iodide (MI) (Rankl et al., 2003)	50.80	50.80	0	0.72	0
1-Brom-naphtalin (1-Bn) (Rankl et al., 2003)	44.40	44.40	0	0	0
Red blood cell (Vijayanand et al., 2005)	36.56	35.20	1.36	0.01	46.2
Platelet (Vijayanand et al., 2005)	118.24	99.14	19.10	12.26	7.44

Table 8. Surface tension parameters (mN/m) of the liquids used for contact angle measurements: total surface tension, γ_{lv} , disperse component of surface tension, $\gamma_{\text{lv}}^{\text{d}}$, polar component of surface tension, $\gamma_{\text{lv}}^{\text{p}}$, electron-donor contribution on polar component, γ_{lv}^- , and electron-acceptor contribution on polar component, γ_{lv}^+

Polymers	Solvents			
	W	G	FA	EG
PSF	79	70	65	60
CMPSF1	78	72	66	57
CMPSF2	73	69	65	54
CMPSF3	71	68	64	52
PSFQ1	64	63	64	51
PSFQ2	64	56	69	48
PSFQ3	32	28	32	29

Table 9. Contact angle of different probe liquids (in °)

Therewith, the relative ratio of the polar component to the total surface tension ranges from approx. 39% for PSF and 43% for CMPSF1, with the substitution degree $\text{DS} < 1$, to 57-61% for CMPSF, with the substitution degree $\text{DS} > 1$, and to 79% for PSFQ. The apolar component, $\gamma_{\text{sv}}^{\text{d}}$, decreases from PSF to CMPSF and PSFQ. The total surface tensions of PSF and CMPSF1, where the substitution degree $\text{DS} < 1$, are dominated by the apolar component, while the total surface tension of CMPSF2, CMPSF3, ($\text{DS} > 1$) and PSFQ are dominated by the

polar term, with the electron donor interactions, γ_{sv}^- , smaller than the electron acceptor ones, γ_{sv}^+ . Thus, the functional groups $-\text{CH}_2\text{Cl}$ attached by chloromethylation process increase the polarity for chloromethylated polysulfones with a substitution degree $\text{DS} > 1$; also, the N, N-dimethylethanolamine side groups introduced by the quaternization process increase the polarity. The change is moderate for chloromethylated polysulfone with $\text{DS} > 1$, with different chloride content.

Samples	GM method			LW/AB method				
	γ_{sv}^d	γ_{sv}^p	γ_{sv}	γ_{sv}^{LW}	γ_{sv}^{AB}	γ_{sv}^-	γ_{sv}^+	$\gamma_{sv}^{LW/AB}$
PSF	17.81	11.21	28.49	18.77	9.34	8.74	28.10	33.23
CMPSF1	16.13	12.32	28.45	21.27	7.46	11.43	28.73	25.97
CMPSF2	13.23	17.56	30.79	16.85	12.38	17.02	29.23	42.35
CMPSF3	12.66	19.43	32.09	15.79	14.14	17.56	29.93	47.23
PSFQ1	8.12	29.88	38.00	12.70	19.29	27.24	31.98	60.31
PSFQ2	8.04	31.11	39.15	8.15	42.56	29.98	43.71	97.38
PSFQ3	8.08	31.20	39.18	7.82	56.82	49.34	64.74	82.70

Table 10. Surface tension parameters (mN/m) for polysulfone (PSF) film, chloromethylated polysulfone films, (CMPSF1, CMPSF2 and CMPSF3) prepared from solutions in chloroform, and quaternized polysulfone films (PSFQ1, PSFQ2 and PSFQ3) prepared from solutions in methanol

Moreover, the surface tension parameters of quaternized polysulfones PSF-DMEA, and PSF-DMOA, with surface properties of water, methylene iodide, 1-brom-naphtalin test liquids from Table 8, and the contact angles measured between these solvents and quaternized polysulfone films from Table 11, are presented in Table 12.

Solvent mixtures	Contact angle		
	W	MI	1-Bn
PSF-DMEA			
100/0 DMF/MeOH	71	28	17
75/25 DMF/MeOH	70	31	22
50/50 DMF/MeOH	61	30	20
25/75 DMF/MeOH	63	31	24
75/25 DMF/water	59	35	21
50/50 DMF/water	60	33	18
40/60 DMF/water	56	33	16
PSF-DMOA			
100/0 DMF/MeOH	72	32	15
75/25 DMF/MeOH	78	32	16
50/50 DMF/MeOH	58	28	16
45/55 DMF/MeOH	77	35	20
75/25 DMF/water	66	34	21
60/40 DMF/water	65	36	25

Table 11. Contact angle ($^\circ$) of different liquids on films prepared from solutions of PSF-DMEA and PSF-DMOA in DMF/MeOH and DMF/water

These parameters are influenced by the solvent/nonsolvent composition from which the films are prepared (Albu et al., 2011; Ioan et al. 2011a). Some studies have reported that the chain shape of a polymer in solution could affect the morphology of the polymer in bulk. In this context, the conformations of both PSF-DMEA and PSF-DMOA are affected by the charged groups from different alkyl radicals of the studied quaternized samples, and also by the composition of the solvent mixtures. For the PSF-DMEA in the DMF/MeOH system, one may observe that the polymer coil dimension decreases with increasing the DMF content in the 0.25–1 volume fraction domain; below a 0.25 volume fraction of DMF, the polymer precipitates. For the same polymer, but in a DMF/water solvent mixture, the dimensions increase with increasing the DMF content, starting from approximately the same volume fraction of DMF. The PSF-DMOA coil dimensions possess maximum values in DMF/MeOH and DMF/water, around 0.6 and 0.8 DMF volume fractions, respectively. For volume fractions of DMF below 0.25 in DMF/MeOH and 0.5 in DMF/water, the PSF-DMOA precipitates due to the nature of the alkyl radicals and content of nonsolvent in the system. Also, the values of intrinsic viscosity are higher for PSF-DMOA - with bulky carbon atoms in the alkyl side chain, compared with PSF-DMEA, where the alkyl side chain possesses two carbon atoms. Therefore, for a given composition of the DMF/MeOH and DMF/water solvent mixtures, one of the components is preferentially adsorbed by the quaternized polysulfone molecules in the direction of a thermodynamically most effective mixture (Filimon et al., 2010). These aspects influence the surface properties of the polymer. PSF-DMEA films possess low polar surface tension parameters, but slightly higher than those for PSF-DMOA. The hydrophobic character is given by the ethyl radical from the N-dimethylethylammonium chloride pendant group and by the octyl radical from the N-dimethyloctylammonium chloride pendant group, respectively.

Solvent mixtures	GM method			LW/AB method				
	γ_{sv}^d	γ_{sv}^p	γ_{sv}	γ_{sv}^{LW}	γ_{sv}^+	γ_{sv}^-	γ_{sv}^{AB}	$\gamma_{sv}^{LW/AB}$
PSF-DMEA, DMF/MeOH								
100/0	43.7	5.9	49.7	42.5	3.6	2.6	6.2	48.7
75/25	42.5	6.6	49.2	41.3	4.3	2.8	6.9	48.1
50/50	42.9	10.7	53.7	41.8	9.9	2.5	9.9	51.7
25/75	42.1	10.0	52.1	40.6	6.5	4.1	10.4	51.0
PSF-DMEA, DMF/water								
75/25	41.8	12.2	54.0	41.5	21.4	0.1	3.18	44.68
50/50	42.6	11.4	54.0	42.3	19.0	0.2	3.83	46.08
40/60	42.8	13.4	56.3	42.7	25.4	0.2	4.15	46.85
PSF-DMOA, DMF/MeOH								
100/0	40.9	5.1	46.0	42.4	0.4	1.4	1.5	43.9
75/25	39.6	3.0	42.6	42.7	0.2	0.8	0.8	43.5
50/50	43.6	1.9	45.2	43.1	1.5	2.0	1.8	44.9
45/55	39.1	3.6	42.7	41.3	1.0	0.5	1.4	42.7
PSF-DMOA, DMF/water								
75/25	38.4	7.5	46.0	41.4	0.5	1.2	1.5	42.9
60/40	38.5	8.6	47.1	40.2	0.8	3.5	3.3	43.6
50/50	41.4	5.9	47.4	42.8	0.5	1.3	1.6	44.4

Table 12. Surface tension parameters (mN/m) for quaternized polysulfone films PSF-DMEA and PSF-DMOA prepared from solutions in DMF/MeOH and DMF/water

Furthermore, the electron donor interactions, γ_{sv}^- , are smaller than the electron acceptor ones, γ_{sv}^+ , for PSF-DMEA, and electron donor interactions, γ_{sv}^- , exceed the electron acceptor interactions, γ_{sv}^+ , for PSF-DMOA, caused by the inductive phenomena from alkyl radical. The results reflect the capacity of the N-dimethylethylammonium chloride or N-dimethyloctylammonium chloride pendant groups to determine the acceptor or donor character of the polar terms, generated by these inductive phenomena.

In the same context, the substitution degrees of polysulfones with bulky phosphorus pendant groups enface the specific properties. Presence of substituted groups in position 1* for samples PS-DOPO-1 and PS-DOPO-2 and in positions 1* and 2* for sample PS-DOPO-3 influence *e.g.* the rheological properties, leading to modification of slopes as a function of viscosity *vs.* substitution degrees, concentration and temperature (Ioan et al., 2011b). This behavior is assigned to the modification of cohesive energy and molar volume for the studied samples. The Arrhenius equation evidenced an increased of activation energy and flow activation entropy, in the following order: PS-DOPO-1 < PS-DOPO-2 < PS-DOPO-3. This implies a higher energy barrier for the movement of an element of the fluid and a more rigid structure for the PS-DOPO3 polymer chain and, as well as, a strong variation with concentration of the activation energy and flow activation entropy. Thus, different forms of the entanglement in polymer solutions are generated by the specific molecular rearrangement of the polysulfone with bulky phosphorus pendant groups with different substitution degrees, at different concentrations and temperatures. Moreover, the viscoelastic characteristics showed that all samples exhibit the behavior characteristic of an elastic gel at high frequencies, when $G' > G''$ and where both moduli are dependent on frequency. These features are characteristic for a physical gel network, in which the gelation process of phosphorus-modified polysulfones is influenced by intramolecular interactions, depending on the substitution degrees and by intermolecular attractions that depend on solution concentration.

Samples	W	F	EG	MI
PS-DOPO-1	77	56	59	43
PS-DOPO-2	78	52	49	21
PS-DOPO-3	82	46	31	≈ 0

Table 13. Contact angle of different probe liquids (water (W), formamide (F), ethylene glycol (EG) and methylene iodide (MI)) in (°) with polysulfones with bulky phosphorus pendant groups

Samples	Surface tension parameters							
	GM method			LW/AB method				
	γ_{sv}^d	γ_{sv}^p	γ_{sv}	γ_{sv}^{LW}	γ_{sv}^{AB}	γ_{sv}^+	γ_{sv}^-	$\gamma_{sv}^{LW/AB}$
PS-DOPO-1	33.18	4.80	37.98	34.23	3.99	0.557	7.15	37.22
PS-DOPO-2	44.62	2.34	46.96	39.20	1.508	0.112	5.063	40.710
PS-DOPO-3	52.85	1.14	53.99	48.85	1.378	0.358	1.327	50.228

Table 14. Surface tension parameters (mN/m) for membranes of PS-DOPO with different substitution degrees, prepared from solutions in DMF

On the other hand, according to Table 13 and, finally, Table 14, all phosphorus-modified polysulfones show low polar surface tension parameters, γ_{sv}^p or γ_{sv}^{AB} , which decrease with increasing the phosphorus pendant groups, and which manifest bring lower contributions to the total surface tension parameters. Furthermore, the electron donor interactions, γ_{sv}^- exceed the electron acceptor interactions, γ_{sv}^+ , considering electron-donor capacity of P=O group. These results show that the studied samples evidence high hydrophobicity, which increases by increasing the substitution degrees. The maximum hydrophobicity of the polysulfones with bulky phosphorus pendant groups would be advantageous, *e.g.*, for dielectric performance, since a low water absorption causes a significant decrease in the dielectric constant and, implicitly, low adhesion to different interfaces.

5. Surface and interfacial free energy of functionalized polysulfones

The effect of different radicals of functionalized polysulfones and of the history of the films formed from solutions on surface properties are analyzed by surface free energy, ΔG_w - expressing the balance between surface hydrophobicity and hydrophilicity (equation (3)) (Faibish et al., 2002; Rankl et al., 2003), by interfacial free energy between two particles of functionalized polysulfones in water phase, ΔG_{sws}^{GM} (equations (4) and (5) or (6)), and by the work of spreading of water, W_s (equation (7)).

$$\Delta G_w = -\gamma_{lv} \cdot (1 + \cos \theta_{water}) \quad (3)$$

where γ_{lv} is given in Tables 8 and θ_{water} is give in Table 9, 11 and 13 for functionalized polysulfones with N,N-dimethylethanolamine (PSFQ), N,N-dimethylethylamine and N,N-dimethyloctylamine (PSF-DMEA and PSF-DMOA), and polysulfones with bulky phosphorus pendant groups (DOPO), respectively.

$$\Delta G_{sws}^{GM} \text{ (or } \Delta G_{sws}^{LW/BAB} \text{)} = -2 \cdot \gamma_{sl} \text{ (or } \gamma_{sl}^{LW/AB} \text{)} \quad (4)$$

$$\gamma_{sl} = \left(\sqrt{\gamma_{lv}^p} - \sqrt{\gamma_{sv}^p} \right)^2 + \left(\sqrt{\gamma_{lv}^d} - \sqrt{\gamma_{sv}^d} \right)^2 \quad (5)$$

$$\gamma_{sl}^{LW/AB} = \left(\sqrt{\gamma_{sv}^d} - \sqrt{\gamma_{lv}^d} \right)^2 + 2 \cdot \left(\sqrt{\gamma_{sv}^+ \cdot \gamma_{sv}^-} + \sqrt{\gamma_{lv}^+ \cdot \gamma_{lv}^-} - \sqrt{\gamma_{sv}^+ \cdot \gamma_{lv}^-} - \sqrt{\gamma_{sv}^- \cdot \gamma_{lv}^+} \right) \quad (6)$$

$$W_s = W_a - W_c = 2 \cdot [(\gamma_{sv}^{LW} \cdot \gamma_{lv}^d)^{1/2} + (\gamma_{sv}^+ \cdot \gamma_{lv}^-)^{1/2} + (\gamma_{sv}^- \cdot \gamma_{lv}^+)^{1/2}] - 2 \cdot \gamma_{lv} \quad (7)$$

Generally, the literature (Faibish et al., 2002; van Oss, 1994) mentions that for $\Delta G_w < -113 \text{ mJ/m}^2$, the polymer can be considered more hydrophilic while, when $\Delta G_w > -113 \text{ mJ/m}^2$, it should be considered more hydrophobic. It is observed from Figure 9 that the surface free energy for PSF and CMPSF samples possesses low wettability. Moreover, Figures 9, 10 and Table 15 show that all functionalized polysulfones are characterized by small wettability, except for PSFQ3, where the hydrophylicity is higher. On the other hand, N,N-dimethyloctylamine groups determine a higher wettability as N,N-dimethylethylamine group (corresponding to PSF-DMOA and PSF-DMEA, respectively) and

these wettability depends on the surface morphology of samples prepared from different composition of DMF/MeOH and DMF/water solvent mixtures (see Table 6). Also, a small difference appears between PS-DOPO samples with different substitution degrees. Thus, one can say that increasing the substitution degrees lead to a slight increase in hydrophobicity.

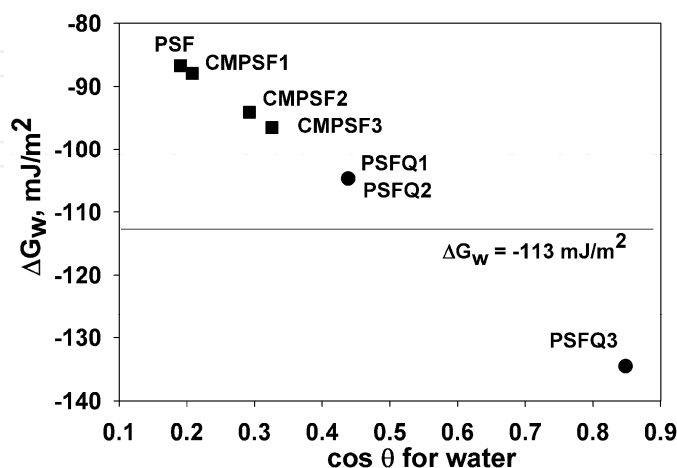


Fig. 9. Surface free energy *vs.* water contact angle for quaternized polysulfones with N,N-dimethylethanolamine

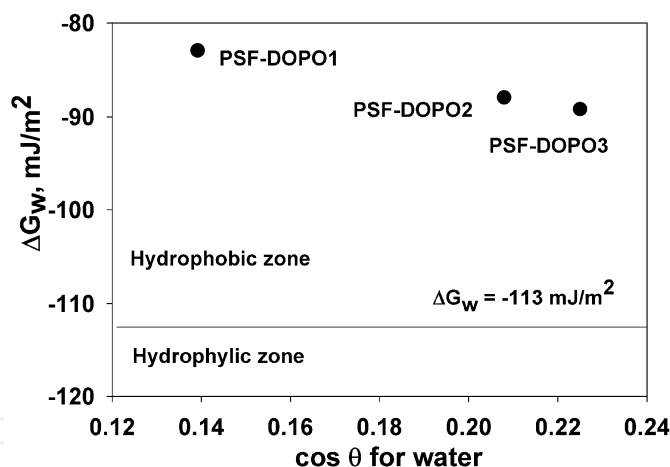


Fig. 10. Surface free energy *vs.* water contact angle for polysulfones with bulky phosphorus pendant groups

The interfacial free energy, ΔG_{sws}^{GM} evaluated from solid-liquid interfacial tension, γ_{sl} , has negative values (see Figure 11 - for PSFQ, Table 15 - for PSF-DMEA and PSF-DMOA, and Table 16 - for PSF-DOPO), indicating an attraction between the two polymer surfaces, *s*, immersed in water, *w*; hence, these materials are considered rather hydrophobic (Dourado et al., 1998; van Oss & Giese, 1995).

In addition, the hydrophobicity of these polymers is described by the work of spreading of water, W_s , over the surface, which represents the difference between the work of water adhesion, W_a , and the work of water cohesion, W_c (equation (7)).

Solvent mixtures	γ_{sl}		ΔG_w		ΔG_{sws}^{GM}	
	DMF/MeOH					
	PSF-DMEA	PSF-DMOA	PSF-DMEA	PSF-DMOA	PSF-DMEA	PSF-DMOA
100/0	25.95	26.92	-67	-95.30	-51.90	-53.84
75/25	24.26	32.06	-68	-87.94	-48.52	-64.12
50/50	18.47	37.15	-75	-111.38	-36.94	-74.30
45/55	-	29.91	-	-89.18	-	-59.82
25/75	19.15	-	-74	-	-38.30	-
DMF/water						
75/25	16.50	21.66	-77	-102.41	-32.30	-43.32
60/40	-	20.08	-	-103.57	-	-40.16
50/50	17.60	25.30	-76	-97.70	-35.20	-50.60
40/60	15.57	-	-79	-	-31.14	-

Table 15. Water interfacial tensions and surface free energy for PSF-DMEA and PSF-DMOA films prepared in different DMF/MeOH and DMF/water, and interfacial free energy between two particles of quaternized polysulfones in water phase

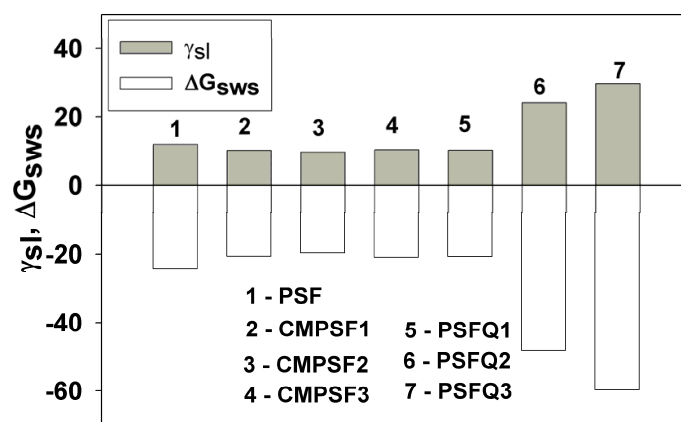


Fig. 11. Water interfacial tensions and surface free energy for polysulfone, chloromethylated polysulfones, and quaternized polysulfones films prepared in DMF/MeOH and DMF/water

Samples	γ_{sl}	$\gamma_{sl}^{LW/AB}$	ΔG_{sws}^{GM}	$\Delta G_{sws}^{LW/AB}$	W_s
PS-DOPO-1	25.69	21.84	-51.38	-43.69	-56.42
PS-DOPO-2	35.54	28.93	-71.08	-57.86	-61.03
PS-DOPO-3	43.65	40.09	-87.30	-80.17	-62.66

Table 16. Solid-water interfacial tensions, γ_{sl} , and interfacial free energy, ΔG_{sws}^{GM} , from the geometrical mean method (GM) and solid-water interfacial tensions, $\gamma_{sl}^{LW/AB}$ and interfacial free energy, $\Delta G_{sws}^{LW/AB}$, from the acid/base method (LW/AB), and the work of spreading of water, W_s , over the polymer surface

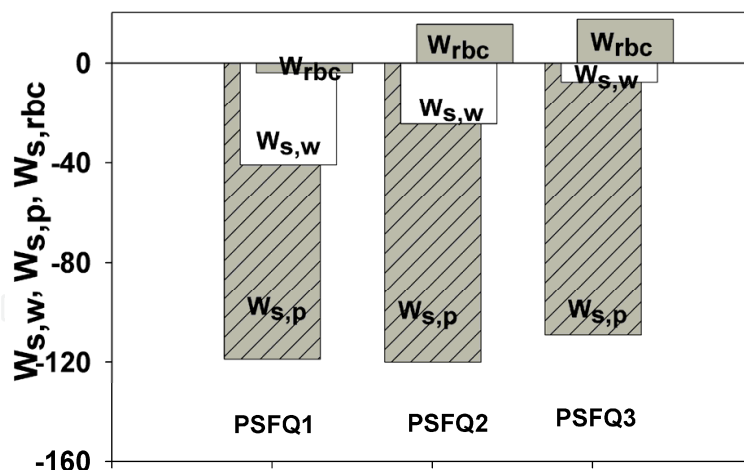


Fig. 12. Work of spreading of water, red blood cells and platelets over the surface of PSFQ1, PSFQ2 and PSFQ3 films

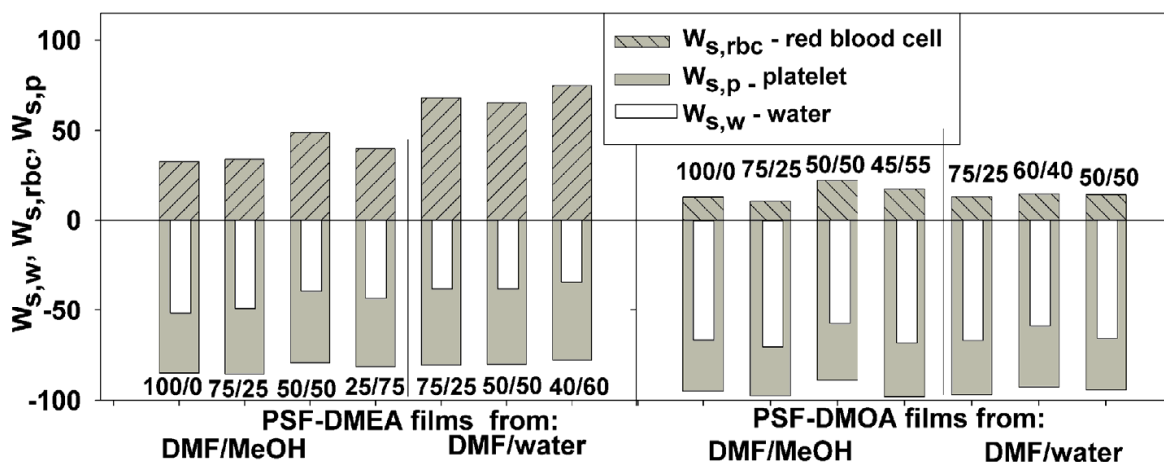


Fig. 13. Work of spreading of water, red blood cells and platelets over the surface of PSF-DMEA and PSF-DMOA films prepared in DMF/MeOH and DMF/water

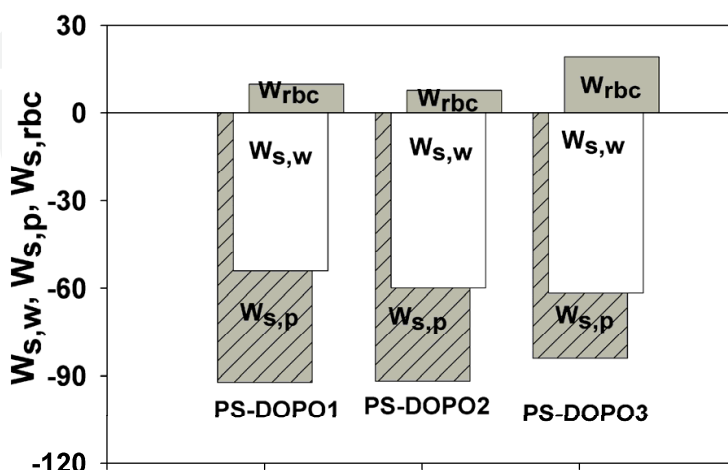


Fig. 14. Work of spreading of water, of red blood cells and of platelets over the surface of PSF-DOPO1, PSF-DOPO2 and PSF-DOPO3 films

According to the negative values of the interfacial free energy of all polysulfone samples, the work of spreading of water, $W_{s,w}$, takes negative values, caused by the hydrophobic surfaces, where the work of water adhesion is low, comparatively with the work of cohesion; at the same time, be noticed that adhesion and implicitly work of spreading of water, W_s , increases with increasing substitution degree for PSFQ samples ($W_{s,w,PSFQ1} < W_{s,w,PSFQ2} < W_{s,w,PSFQ3}$), is lower for PSF-DMOA than for PSF-DMEA, and decreases with increasing of substitution degrees for PSF-DOPO ($W_{s,w,PS-DOPO1} < W_{s,w,PS-DOPO2} < W_{s,w,PS-DOPO3}$).

6. Blood - functionalized polysulfone interactions

Blood compatibility is dictated by the manner in which their surfaces interact with blood constituents, like red blood cells and platelets. To analyze the possibilities of using the functionalized polysulfones in biomedical applications, and for establishing its compatibility with blood, equation (7) is used, where $W_{s,rbc}$ and $W_{s,p}$ describe the work of spreading of red blood cells and platelets (Vijayanand et al., 2005); when blood is exposed to a biomaterial surface, adhesion of cells occurs and the extent of adhesion decides the life of the implanted biomaterials; thus, cellular adhesion to biomaterial surfaces could activate coagulation and the immunological cascades. Therefore, cellular adhesion has a direct bearing on the thrombogenicity and immunogenicity of a biomaterial, and thus dictates its blood compatibility. The work of adhesion of the red blood cells can be considered as a parameter for characterizing biomaterials *versus* cell adhesion. The materials which exhibit a lower work of adhesion would lead to a lower extent of cell adhesion than those with a higher work of adhesion. Considering the surface energy parameters (γ_{lv} , γ_{lv}^d , γ_{lv}^+ , γ_{lv}^-) given in Table 8 for red blood cells and platelets, the work of spreading of blood cells and platelets is estimated by equation (7), with surface tension parameters listed in Table 10 for PSFQ, Table 12 for PSF-DMEA and PSF-DMOA, and in Table 14 for PSF-DOPO.

Figures 12, 13 and 14 show positive values for the work of spreading of red blood cells, $W_{s,rbc}$, and negative values for the work of spreading of platelets, $W_{s,p}$, suggesting a higher work of adhesion comparatively with that of cohesion for the red blood cells, but a smaller work of adhesion comparatively with the one of cohesion for platelets. Among these polysulfones, the work of spreading of red blood cells, $W_{s,rbc}$ exhibits a negative value for the PSFQ1, generated by lower hydrophobicity, and a highest value for the PSF-DMEA, characterized by high disperse parameter of surface tension.

These results suggest that the exposure of platelets to functionalized polysulfone films determines an increase of platelets cohesion, and that a good hydrophobicity can be correlated with a good adhesion of the red blood cells on the surface of the polysulfone films.

In summary, both red blood cells and platelets are extremely important in deciding the blood compatibility of a material. Moreover, it is known that adhesion of the red blood cells onto a surface, *e.g.* modified polysulfones, requires knowledge of the interactions with the vascular components. Thus, endothelial glycocalyx along with the mucopolysaccharides adsorbed to the endothelial surface of the vascular endothelium reject clotting factors and

platelets - which have a significant role in thrombus formation (Reitsma et al., 2007). In this context, adhesion of the red blood cells and cohesion of platelets to surface films must be discussed in correlation with future specific biomedical applications. These results seem to be applicable for evaluating bacterial adhesion to the surfaces, and could be subsequently employed for studying possible implanted induced infections, or for obtaining semipermeable membranes.

7. Antimicrobial activity assessments

The literature shows that quaternary ammonium salts represent one of the most popular types of antimicrobial agents (Hazziza-Laskar et al., 2005; Xu et al., 2006; Yu et al., 2007; Merianos, 1991). Their biological activity, depending on their structure and physico-chemical properties, affects the interaction with the cytoplasmic membrane of bacteria and influences cell metabolism.

The antimicrobial activity of quaternized polysulfones with various ionic chlorine contents, in DMSO, at different concentrations, is investigated against *Escherichia coli* (*E. coli*) and *Staphylococcus aureus* (*S. aureus*). As shown in Figure 15 and Table 17, these polymers inhibit the growth of microorganisms, the inhibition becoming stronger with increasing the polycationic nature of the modified polysulfone and with the polymer solution concentration. Also, for all solutions, the inhibition is intense compared to DMSO, which is used as a control sample.

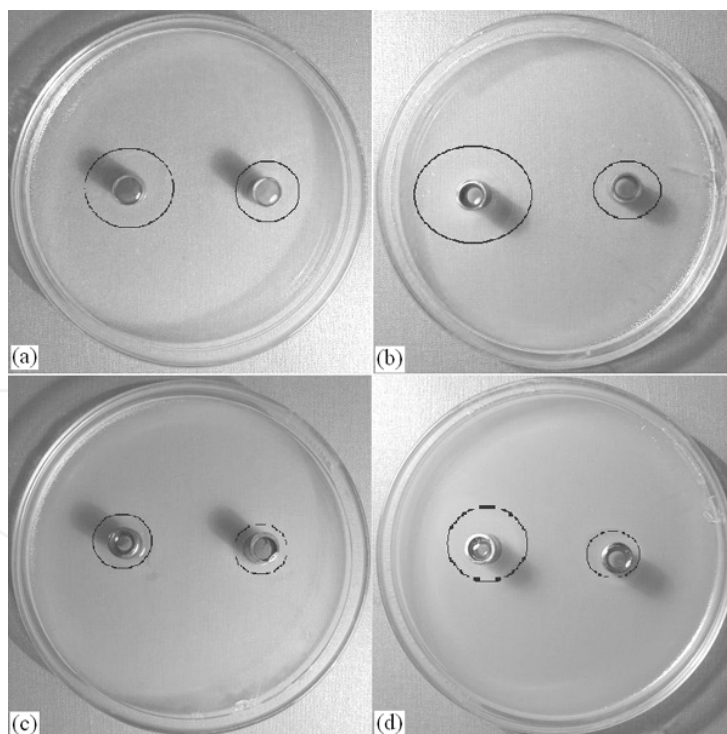


Fig. 15. Antimicrobial screening tests: (a) PSFQ1 in DMSO, $c = 1.08$ g/L, against *Escherichia coli*; (b) PSFQ2 in DMSO, $c = 1.10$ g/L, against *Escherichia coli*; (c) PSFQ1 in DMSO, $c = 1.08$ g/L, against *Staphylococcus aureus*; (d) PSFQ2 in DMSO, $c = 1.10$ g/L, against *Staphylococcus aureus*. In each figure, the inhibition area on the right side is recorded for DMSO as a control sample

Microorganism	PSFQ1		PSFQ2		Control (DMSO)
	0.52 g/L	1.08 g/L	0.52 g/L	1.1 g/L	
<i>E. coli</i>	13	19	22	23	12
<i>S. aureus</i>	11	13	15	18	10

Table 17. Antimicrobial activity expressed by the diameter of the inhibition zone (mm) of PSFQ1 and PSFQ2 in DMSO at two concentrations and of DMSO used as a control sample against *Escherichia coli* and *Staphylococcus aureus*

The cationic modified polysulfones with quaternary ammonium group interfere with the bacterial metabolism by electrostatic stacking at the cell surface of the bacteria (Xu et al., 2006). This conclusion is evaluated in terms of the diameter of the inhibition zone presented in Table 17. The results show that the bacterial activity of the tested compounds is dependent on the microorganism nature. Thus, the *E. coli* is found to be much more sensitive to the investigated polymers than the *S. aureus*.

On the other hand, the differences in the composition of the cell wall of Gram-negative (*E. coli*) and Gram-positive (*S. aureus*) bacteria cause different resistance to killing by antimicrobial agents. It is known that the component of Gram-positive bacteria cell walls is peptidoglycan, whereas the major constituents of Gram-negative bacteria cell walls are peptidoglycan, together with other membranes, such as lipopolysaccharides and proteins. These components of the cell walls generate the hydrophilic character of *E. coli* bacteria and the hydrophobic character of *S. aureus*. Thus, the different inhibiting effects of PSFQ1 and PSFQ2 on the growth of the tested *E. coli* and *S. aureus* bacteria may be due to different antimicrobial activities.

Therefore, all these aspects indicate that the antimicrobial activity depends not only on the substituent groups of the quaternized polysulfones but also on the hydrophilic or hydrophobic character of the bacteria, which generated different interactions of the quaternary ammonium salt groups with the bacterial cell membrane. In particular, the adhesion of the relatively hydrophilic *E. coli* to the hydrophilic quaternized polysulfones is higher than the adhesion of hydrophobic *S. aureus* cells.

8. Conclusion

New quaternized polysulfones, prepared by quaternization of chloromethylated polysulfone with N,N-dimethylethanolamine, N,N-dimethylethylamine, N,N-dimethyloctylamine and also polysulfones with bulky phosphorus pendant groups, obtained by chemical modification of the chloromethylated polysulfones by reacting the chloromethyl group with the P-H bond of 9,10-dihydro-oxa-10-phosphophenanthrene-10-oxide are investigated to obtain information on their hydrophilic/hydrophobic properties and blood compatibility. The history of the formed films, prepared by a dry-cast process in pure solvents or in different solvent/nonsolvent mixtures, influenced the surface tension parameters, surface and interfacial free energy and the work of spreading of water, maintaining the surfaces hydrophobic characteristics of polysulfones. On the other hand, the results reflect the capacity of N-dimethylethanolammonium chloride pendant group to determine the acceptor character of the polar terms, capacity of N-dimethylethylammonium or N-dimethyloctylammonium chloride pendant groups to determine the acceptor or donor

character of the polar terms, and capacity of P-H bond of 9,10-dihydro-oxa-10-phosphophenanthrene-10-oxide to determine the donor character of the polar terms, caused by the inductive phenomena of different pendant groups.

The AFM images show that surface morphology is characterized by roughness and nodules formations, depending on the composition of solvent/nonsolvent mixtures, including the characteristics of polysulfones and the thermodynamic quality of the solvents. Moreover, the results suggest that:

- surface hydrophobicity and surface roughness are the parameters controlling the compatibility with the red blood cells and platelets: a good hydrophobicity can be correlated with a good adhesion of the red blood cells and with a good cohesions of the platelets on the surface of the polysulfone films;
- high work of adhesion comparatively with work of cohesion for the red blood cells, but a smaller work of adhesion comparatively with the one of cohesion for platelets is obtained. Among these polysulfones, the work of spreading of red blood cells, $W_{s,rbc}$ exhibits a negative value for the quaternized polysulfone with N,N-dimethylethanolamine pendant group and 2.15 ionic chlorine content (PSFQ1), generated by lower hydrophobicity, and a highest value for the quaternized polysulfone with N,N-dimethylethylamine pendant group (PSF-DMEA), characterized by high disperse parameter of surface tension.

On the other hand, the antimicrobial activity of polysulfones with quaternary ammonium groups is considered to be one of the important properties that are directly related to new possible applications. In this study, adhesion of *Escherichia coli* and *Staphylococcus aureus* cells to PSFQ is investigated. These polymers inhibit the growth of microorganisms, with inhibition becoming stronger with the increasing polycationic nature of the modified polysulfone and the concentration of the polymer solution. Moreover, the adhesion of the relatively hydrophilic *E. coli* to hydrophilic quaternized polysulfone is higher than the adhesion of the hydrophobic *S. aureus* cells.

These results are useful in investigations on specific biomedical applications, including evaluation of bacterial adhesion to the surfaces, and utilization of modified polysulfones as semipermeable membranes.

9. References

- Albu, R.M.; Avram, E.; Stoica, I.; Ioanid, E.G.; Popovici, D. & Ioan, S. (2011). Surface Properties and Compatibility with Blood of New Quaternized Polysulfones. *Journal of Biomaterials and Nanobiotechnology*, Vol.2, No.2, (April 2011), pp. 114-123, ISSN 2158-7027
- Barikani, M. & Mehdipour-Ataei, S. (2000). Synthesis, Characterization and Thermal Properties of Novel Arylene Sulfone Ether Polyimides and Polyamides. *Journal of Polymer Science, Part A: Polymer Chemistry*, Vol.38, No.9, (May 2000), pp. 1487-1492, ISSN 1099-0518
- Della Volpe, C.; Maniglio, D.; Brugnara, M.; Siboni, S. & Morra, M. (2004). The Solid Surface Free Energy Calculation: in Defense of the Multicomponent Approach. *Journal of*

- Colloid and Interface Science*, Vol.271, No.2, (March 2004), pp. 434-453, ISSN 0021-9797
- Dourado, F.; Gama, F.M.; Chibowski, E. & Mota, M. (1998). Characterization of Cellulose Surface Free Energy. *Journal of Adhesion Science and Technology*, Vol.12, No.10 (November 1998), pp. 1081-1090, ISSN 0169-4243
- Faibish, R.S.; Yoshida, W. & Cohen, Y. (2002). Contact Angle Study on Polymer-Grafted Silicon Wafers. *Journal of Colloid and Interface Science*, Vol.256, No.2, (February 2003), pp. 341-350, ISSN 0021-9797
- Filimon, A.; Albu, R.M.; Avram, E. & Ioan, S. (2010). Effect of Alkyl Side Chain on the Conformational Properties of Polysulfones with Quaternary Groups. *Journal of Macromolecular Science, Part B: Physics*, Vol.49, No.1, (January 2010), pp. 207-217, ISSN 0022-2348
- Filimon, A.; Avram, E.; Dunca, S.; Stoica, I. & Ioan, S. (2009). Surface Properties and Antibacterial Activity of Quaternized Polysulfones. *Journal of Applied Polymer Science*, Vol.112, No.3, (February 2009), pp. 1808-1816, ISSN 1097-4628
- Filimon, A.; Avram, E. & Ioan, S. (2007). Influence of Mixed Solvents and Temperature on the Solution Properties of Quaternized Polysulfones. *Journal of Macromolecular Science, Part B: Physics*, Vol.46, No.3 (March 2007), pp. 503-520, ISSN 0022-2348
- Guan, R.; Zou, H.; Lu, D.; Gong, C. & Liu, Y. (2005). Polyethersulfone Sulfonated by Chlorosulfonic Acid and its Membrane Characteristics. *European Polymer Journal*, Vol.41, No. 7, (July 2005), pp. 1554-1560, ISSN 0014-3057
- Guiver, M.D.; Black, P.; Tam, C.M. & Deslandes, Y. (1993). Functionalized Polysulfone Membranes by Heterogeneous Lithiation. *Journal of Applied Polymer Science*, Vol.48, No.9, (June 1993), pp. 1597-1606, ISSN 1097-4628
- Hazziza-Laskar, J.; Helary, G. & Sauvet, G. (2005). Biocidal Polymers Active by Contact. IV. Polyurethanes Based on Polysiloxanes with Pendant Primary Alcohols and Quaternary Ammonium Groups. *Journal of Applied Polymer Science*, Vol.58, No.1, (October 2005), pp. 77-84, ISSN 1097-4628
- Higuchi, A.; Iwata, N.; Tsubaki, M. & Nakagawa, T. (1988). Surface-Modified Polysulfone Hollow Fibers. *Journal of Applied Polymer Science*, Vol.36, No.8, (October 1988), pp. 1753-1767, ISSN 1097-4628
- Higuchi, A.; Shirano, K.; Harashima, M.; Yoon, B.O.; Hara, M.; Hattori M. & Imamura, K. (2002). Chemically Modified Polysulfone Hollow Fibers with Vinylpyrrolidone Having Improved Blood Compatibility. *Biomaterials*, Vol.23, No.13, (July 2002), pp. 2659-2666, ISSN 0142-9612
- Hopkins, A.R.; Rasmussen, P.G.; Basheer, R.A. (1996). Characterization of Solution and Solid State Properties of Undoped and Doped Polyanilines Processed from Hexafluoro-2-Propanol. *Macromolecules*, Vol.29, No.24, (November 1996), pp. 7838-7846, ISSN 0024-9297
- Huang, D.H.; Ying, Y.M. & Zhuang, G.Q. (2000). Influence of Intermolecular Entanglements on the Glass Transition and Structural Relaxation Behaviors of Macromolecules. 2. Polystyrene and Phenolphthalein Poly(ether sulfone). *Macromolecules*, Vol. 33, No. 2, (January 2000), pp. 461-464, ISSN 0024-9297
- Idris, A.; Zaina, N.M. & Noordinb, M.Y. (2007). Synthesis, Characterization and Performance of Asymmetric Polyethersulfone (PES) Ultrafiltration Membranes with Polyethylene Glycol of Different Molecular Weights as Additives. *Desalination*, Vol.207, No.1-3, (March 2007), pp. 324-339, ISSN 0011-9164

- Ioan, S.; Albu, R.M.; Avram, E.; Stoica, I. & Ioanid, E.G. (2011a). Surface Characterization of Quaternized Polysulfone Films and Biocompatibility Studies. *Journal of Applied Polymer Science*, Vol.121, No.1, (July 2011), pp. 127-137, ISSN 1097-4628
- Ioan, S.; Buruiana, L.I.; Petreus, O.; Avram, E.; Stoica, I. & Ioanid, G.E. (2011b). Rheological and Morphological Properties of Phosphorus-Containing Polysulfones. *Polymer-Plastics Technology and Engineering*, Vol.50, No.1, (January 2011), pp. 36-46, ISSN 0360-2559
- Ioan, S.; Filimon, A. & Avram, E. (2006a). Influence of the Degree of Substitution on the Solution Properties of Chloromethylated Polysulfone. *Journal of Applied Polymer Science*, Vol.101, No.1, (April 2006), pp. 524-531, ISSN 1097-4628
- Ioan, S.; Filimon, A. & Avram, E. (2006b). Conformation and Viscometric Behavior of Quaternized Polysulfone in Dilute Solution. *Polymer Engineering Science*, Vol.46, No.7, (May 2006), pp. 827-836, ISSN 1548-2634
- Ioan, S.; Filimon, A.; Avram, E. & Ioanid, G. (2007). Effect of Chemical Structure and Plasma Treatment on the Surface Properties of Polysulfones. *e-Polymers*, No.031, (March 2007), pp. 1- 13, ISSN 1618-7229
- Johnson, R.N. (1969). Polysulfones. Plastics, Resins, Rubbers, Fibers, In: *Encyclopedia of Polymer Science and Technology*, F.M. Herman, G.G. Norman & M.N. Bikales, (Eds.), 447-463, John Wiley & Sons, New York, London, Sydney & Toronto
- Kälble, D.H. (1969). Peel Adhesion: Influence of Surface Energies and Adhesive Rheology. *Journal Adhesion*, Vol.1, No.2, (April 1969), pp. 102-123, ISSN 0021-8464
- Khang, G.; Lee H.B. & Park, J.B. (1995). Biocompatibility of Polysulfone. I. Surface Modifications and Characterizations. *Biomedical Materials and Engineering*, Vol.5, No.4, (April 1995), pp. 245-258, ISSN 0959-2989
- Kesting, R.E. (1990). The Four Tiers of Structure in Integrally Skinned Phase Inversion Membranes and Their Relevance to the Various Separation Regimes. *Journal of Applied Polymer Science*, Vol.41, No.11-12, (December 1990), pp. 2739-2752, ISSN 1097-4628
- Kochkodan, V.; Tsarenko, S.; Potapchenko, N.; Kosinova, V. & Goncharuk, V. (2008). Adhesion of Microorganisms to Polymer Membranes: a Photobactericidal Effect of Surface Treatment with TiO₂. *Desalination*, Vol.220, No.1-3, (March 2008), pp. 380-385, ISSN 0011-9164
- Kwok, D.Y.; Ng, H. & Neumann, A.W. (2000). Experimental Study on Contact Angle Patterns: Liquid Surface Tensions Less than Solid Surface Tensions. *Journal of Colloid and Interface Science*, Vol.225, No.2, (March 2004), pp. 323-328, ISSN 0021-9797
- Luca, C.; Avram, E. & Petrariu, I. (1988). Quaternary Ammonium Polyelectrolytes. V. Amination Studies of Chloromethylated Polystyrene with N,N-Dimethylalkylamines. *Journal of Macromolecular Science, Part A: Pure Applied Chemistry*, Vol.25, No.4, (April 1988), pp. 345-361, ISSN 1520-5738
- Mann, B.K. & West, J.L. (2001). Tissue Engineering in the Cardiovascular System: Progress Toward a Tissue Engineered Heart. *The Anatomical Record*, Vol.263, No.4, (August 2001), pp. 367-371, ISSN 1932-8494
- Merianos, J.J. (1991). Quaternary Ammonium Antimicrobial Compounds, In: *Disinfection, Sterilization and Preservation*. Block, S.S., pp. 225, Lea & Febiger, Philadelphia
- Owens, D.K. & Wend, R.C. (1969). Estimation of the Surface Free Energy of Polymers. *Journal of Applied Polymer Science*, Vol.13, No.8, (August 1969), pp. 1741-1747, ISSN 1097-4628

- Petreus, O.; Avram, E. & Serbezeanu, D. (2010). Synthesis and Characterization of Phosphorus-Containing Polysulfone. *Polymer Engineering Science*, Vol.50, No.1, (January 2010), pp. 48-56, ISSN 1548-2634
- Qian, J.W.; An, Q.F.; Wang, L.N.; Zhang, L. & Shen, L. (2005). Influence of the Dilute-Solution Properties of Cellulose Acetate in Solvent Mixtures on the Morphology and Pervaporation Performance of their Membranes. *Journal of Applied Polymer Science*, Vol.97, No.5, (September 2005), pp. 1891-1898, ISSN 1097-4628
- Rankl, M.; Laib, S. & Seeger, S. (2003). Surface Tension Properties of Surface-Coatings for Application in Biodiagnostics Determined by Contact Angle Measurements. *Colloids and Surface B: Biointerfaces*, Vol.30, No.3, (July 2003), pp. 177-186, ISSN 0927-7765
- Reitsma, S.; Slaaf, D.W.; Vink, H.; van Zandvoort, M.A.M.J. & oude Egbrink, M.G.A. (2007). The Endothelial Glycocalyx: Composition, Functions, and Visualization. *Pflügers Archiv - European Journal of Physiology*, Vol.454, No.3, (June 2007), pp. 345-359, ISSN 0031-6768
- Ström, G.; Fredriksson, M. & Stenius, P. (1987). Contact Angles, Work of Adhesion, and Interfacial Tensions at a Dissolving Hydrocarbon Surface. *Journal of Colloid and Interface Science*, Vol.119, No. (2), (October 1987), pp 352-361, ISSN 0021-9797
- Tomaszewska, M.; Jarosiewicz, A. & Karakulski, K. (2002). Physical and Chemical Characteristics of Polymer Coatings in CRF Formulation. *Desalination*, Vol.146, No.1-3, (September 2002), pp. 319-323, ISSN 0011-9164
- van Oss, C.J.; Good R.J. & Chaudhury, M.K. (1988a). Additive and Nonadditive Surface Tension Components and the Interpretation of Contact Angles. *Langmuir*, Vol.4, No.4, (July 1988), pp. 884-891, ISSN 743-7463
- van Oss, C.J.; Ju, L.; Chaudhury, M.K. & Good, R.J. (1988b). Interfacial Lifshitz-van der Waals and Polar Interactions in Macroscopic Systems. *Chemical Reviews*, Vol.88, No.6, (September 1988), pp. 927-941, ISSN 0009-2665
- van Oss, C.J.; Ju, L.; Chaudhury, M.K. & Good, R.J. (1989). Estimation of the Polar Parameters of the Surface Tension of Liquids by Contact Angle Measurements on Gels. *Journal of Colloid and Interface Science*, Vol.128, No.2, (March 1989), pp. 313-319, ISSN 0021-9797
- van Oss, C.J. & Giese, R.F. (1995). The Hydrophilicity and Hydrophobicity of Clay Minerals. *Clay Clay Miner*, Vol.43, No.4, (April 1995), pp. 474-477, ISSN 0009-8558
- Vijayanand, K.; Deepak, K.; Pattanayak, D.K.; Rama Mohan, T.R. & Banerjee, R. (2005). Interpenetrating Blood-Biomaterial Interactions from Surface Free Energy and Work of Adhesion. *Trends in Biomaterials and Artificial Organs*, Vol.18, No.2, (January 2005), pp. 73-83, ISSN 0971-1198
- Xu, X. ; Li, S. ; Jia, F. & Liu, P. (2006). Synthesis and Antimicrobial Activity of Nano-fumed Silica Derivative with N,N-Dimethyl-n-Hexadecylamine. *Life Science Journal*, Vol.3, No.1, (January 2006), pp. 59-62, ISSN 1097-8135
- Yildirim, E. (1997) Polymer Adsorption, In: *Handbook of Surface and Colloid Chemistry*, Birdi, K.S., pp. 266-307, CRC Press, ISBN 0-8493-945-7, Boca Raton
- Yu, H.; Huang, Y.; Ying, H. & Xiao, C. (2007). Preparation and Characterization of a Quaternary Ammonium Derivative of Konjac Glucomannan. *Carbohydrate Polymers*, Vol.69, No.1, (May 2007), pp. 29-40, ISSN 0144-8617

© 2012 The Author(s). Licensee IntechOpen. This is an open access article distributed under the terms of the [Creative Commons Attribution 3.0 License](#), which permits unrestricted use, distribution, and reproduction in any medium, provided the original work is properly cited.

IntechOpen

IntechOpen